# Mesoscopic P-wave attenuation model to estimation of free gas saturation

Francisco Cabrera, University of Pamplona – Colombia
Flor A. Vivas, German D. Camacho, Herling Gonzalez, Colombian Institute of Petroleum-Ecopetrol



### Abstract

We combine the mesoscopic P-wave attenuation model of double porosity and a frequency-based method for measuring seismic attenuation to predict the gas saturation petrophysical parameter. The ongoing case study is related to a free gas layer associated to a hydrate gas, which produce a reflection of high amplitude and inverse polarity detected in the seismic profile. Partial results of methodology application are presented.

### Introduction

We present the joint application of processing, modeling and inversion to estimation of petrophysical parameters using the mesoscopic model of attenuation to a biphasic media. The objective is applied the methodology proposed by Morgan et al. (2012) to estimate the gas saturation associated to a seismic line with a Bottom Simulating Reflector (BSR) related to hydrate methane.

The gas saturation is a petrophysical parameter required to evaluate the reservoir potential and usually is based in direct measurements. Exploration of areas with little or no in situ information require the developing of techniques based on seismic data to make the first estimate of reserves.

This work is based in the assumption that the cause of high amplitude of the BSR associated to the hydrate gas is the free gas trapped below of that. The inversion of impedance produces the inversion in polarity between the Bottom Reflector (BS) and the BSR (Kumar and Rajput, 2011).

Map the BSR in the seismic profile is the first approximation to map the extension of free gas distribution. After that, estimation of energy attenuation in the free gas layer must be used to evaluate the petrophysical parameters.

The estimation of free gas saturation through the velocities inversion is reported very sensitive (Zillmer, 2006), whereas the attenuation and dispersion of velocities are reported as properties strong related to the saturation fluid in the porous rock.

In this work we present the advance in applied the methodology proposed by Morgan et al., (2012), using the mesoscopic model of attenuation to a periodic layer of water and gas (Carcione and Picotti, 2006). This methodology can be extending to different fluid saturation in other exploration problems.

### Q estimation from seismic data

Attenuation is classified as intrinsic and apparent, and the dimensionless quantity that measures the amplitude attenuation is represented by the quality factor *Q*.

The apparent attenuation $Q_{app}$ is related to wave amplitude decrease in layered media, associated with the phenomena of reflection, transmission, multiples, mode conversion and random scattering (Liner, 2012).

The intrinsic attenuation $Q_i$ represents the loss energy in the rock effect of slightly inelastic behavior of the rock skeleton, fluid movement in the porous media and friction between grains or crack faces (Dvorkin and Nur, 1993).

The effective attenuation is represented by

$$\frac{1}{Q_{eff}} = \frac{1}{Q_i} + \frac{1}{Q_{app}}.$$

In this work we consider that the measurements of attenuation from seismic data are produced fundamentally by the intrinsic effect of fluid flow and are disregarding the loss by apparent attenuation.

The fluid flow is considered the intrinsic effect to P-wave attenuation of major importance below 1 KHz (Muller et al., 2010). The model that best reproduces the observed level of attenuation produced by wave-induced fluid flow through a partially saturated porous media is the mesoscopic scale model of the in homogeneities, which will be explained in the next section.

To measure the intrinsic attenuation, from a core in the laboratory, a plot of strain-stress for a sinusoidal stress of frequency $\omega$ is made. A curve of elliptical shape is obtained, whose area is determined by the phase shift $\delta$ between stress and strain. The energy loss per cycle $\Delta E$ is proportional to the area enclosed by the curve, for this reason $\delta$ is named the loss angle. The quality factor *Q* is defined as

$$Q(\omega) = {}^{1}/_{\tan(\delta)}, \text{ or} \quad (1)$$

$$\frac{1}{Q(\omega)} = -\frac{1}{\pi}\frac{\Delta E}{E},$$

where *E* corresponds to the peak of energy stored in the volume (Aki, 1980). Figure 1 represents the inverse relation between the loss angle and a quality factor *Q*.

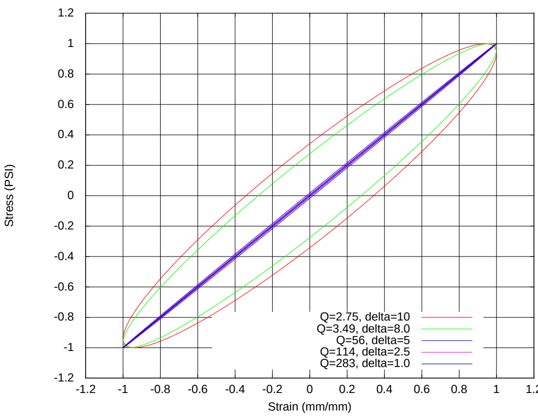


Figure 1: Strain-stress relation for a sinusoidal stress. Values of Q equal to 2.75, 3.49, 56, 114 and 283.

To estimate *Q* from seismic data, we need to observe the exponential amplitude decay in the time interval $\Delta t$ in a seismic trace. To a fixed frequency we can write

$$A(f) = A_0(f)e^{-\frac{\pi\Delta t}{Q(f)}f}, \text{ or}$$

$$ln\left(\frac{A(f)}{A_0(f)}\right) = -\frac{\pi\Delta t}{Q(f)}f. \quad (2)$$

Under the assumption that the attenuation is constant in the range of frequency analyzed, a linear regression can be used in Equation 2 to obtain an estimate value of Q. This process is made to each trace and each interval $\Delta t$ analyzed.

To guarantee that the signal has enough time separation for attenuation estimate, we use the BSR horizon as reference to the amplitude $A_0(f)$ and calculated the two wave travel time (*TWT*) for the wavelength corresponding to the frequency with most energy in this region. For 16 Hz frequency component and using the velocity of 1500 m/s, see Figure 2, we calculated 125 ms to the *TWT*. For this reason, $A(t)$ was measured at a horizon around 125 ms below the BSR.

Figure 3 shows a zoom of a stack section where the BSR has the higher amplitudes. We use the BSR to pick the top horizon and the bottom horizon around 125ms below, in this window is make the attenuation analysis.

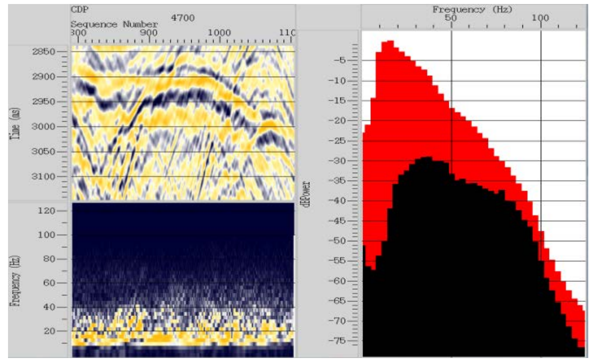


Figure 2: Spectral analysis around BSR location. 16 Hz corresponds to the most energy frequency.

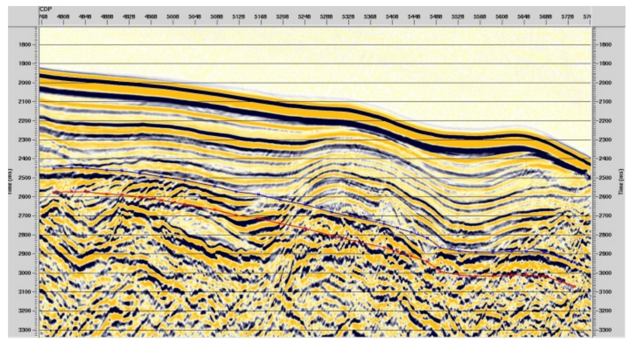

Figure 3: Stack seismic section with BSR horizon (blue) and bottom horizons (red) to the *Q* estimation.

### Mesoscopic attenuation model

Gas saturation can be measure using velocity propagation of P and S waves or attenuation them. The attenuation is strong related to the petrophysical properties of the fluids and skeleton such as porosity, permeability, viscosity, and the saturation of the fluids.

The model that explains the attenuation of P and S waves in the low frequency range of interest to seismic exploration is the mesoscopic model of attenuation and dispersion. The term mesoscopic made reference to a scale intermediated between the scale of the wavelength (tens of meters) and the scale of the pores in the rock (micrometers). The mesoscopic scale is described as the scale of the heterogeneities or patches of fluids and fractures (centimeters).

White (1975) developed the model of partial saturation in a media building with bubbles of gas rounded by rings saturated by other fluid. White´s model to a heterogeneous media shows that the attenuation is related to the effective bulk modulus K. The effective modulus is complex and reproduces the dependence with frequency of the velocity and attenuation. White´s model then reproduce dispersion and attenuation of waves.

The mesoscopic models (Pride et al., 2004; Jhonson, 2001) show that main cause of attenuation and dispersion of the P and S waves in a biphasic media is the fluid flow produced by the gradient of pressure. The gradient of pressure can be produced by the difference in the lithology of the two porous media with the same saturation fluid or/and by the difference in the saturation fluid in the same lithology.

The mesoscopic model proposed by Carcione and Picotti (2006) establish a functional relation between the petrophysical parameters of two porous saturated media and the attenuation or quality factor *Q*.

To purposes of this work, we modeled the layer of free gas as only one lithology with two saturation fluid: gas $S_g$ and water $S_w$. The model corresponds to a periodic system of two layers with thickness $d_1$ and $d_2$ to water and gas, respectively, see Figure 4.


Figure 4: Representation of periodic layers to mesoscopic model of heterogeneities.

Defining the variables *P* and *W*, as the pressure and flow of fluid, and taking spatial dependence with depth (z) and time dependence in the way $e^{-i\omega t}$, the following system of equation must be satisfied:

$$\frac{dP}{dz} = -\left(\frac{\eta}{\kappa}\right)W, \qquad (3)$$

$$\frac{dW}{dz} = \frac{i\omega\alpha}{K + \frac{4}{3}\mu}\left(\frac{P}{R} - 1\right).$$

Taking $L = d_1 + d_2$, and applying the periodic and continuity boundary conditions

$$P(0) = P(L), W(0) = W(L), \text{ and}$$

$$P_1(d_1) = P_2(d_1),\ W_1(d_1) = W_2(d_1),$$

we can find the bulk modulus to the equivalent media (Norris, 1993) as function of pressure as

$$C^* = \langle\frac{1-\alpha P}{K+\frac{4}{3\mu}}\rangle^{-1}, \qquad (4)$$

where the symbol <> meaning the weight average value taken over one period *L,* assuming the mesoscopic scale condition $L \ll \lambda$.

In this model the complex velocity is defined as

$$V^* = \sqrt{\frac{C^*}{<\rho>}}, \qquad (5)$$

where $< \rho >$ is the equivalent density for the two media.

The loss angle is given by the equation

$$\delta = tan^{-1}\left(\frac{RealV^{*2}}{ImagV^{*2}}\right), \text{ or} \qquad (6)$$

$$Q(\omega) = {}^1\!/_{\tan(\delta)} = \frac{ImagV^{*2}}{RealV^{*2}}. \qquad (7)$$

Under flow null and constant pressure conditions, the bulk modulus, given by Equation 4, is real and frequency independent. Then, the phase velocity, given by Equation 5, is independent of frequency too, and according to Equation 6, the attenuation is null.

With the purpose to write the functional relation of *Q* with the petrophysical parameters, we must find the expression of the pressure *P*. The system of two differential equations, given by Equations 3, is rewriting as the second order differential equation:

$$\frac{d^2P}{dz^2} + AR^{-1}P = A, \qquad (7)$$

where A and R are constants in each layer of the periodic system, to j= 1,2

$$A_j = \left(\frac{\eta_j}{\kappa_j}\right)\frac{i\omega}{K_{mj}+\frac{4}{3\mu_j}},\ R_j = \frac{\alpha_j M_j}{K_{cj}+\frac{4}{3\mu_j}}, \qquad (8)$$

Solution of Equation 7 is given by

$$P_j = c_{1j}\cos\left(\frac{d_j Z_j}{L_j}\right) + c_{2j}\cos\left(\frac{d_j Z_j}{L_j}\right) + R_j, \qquad (9)$$

with

$$Z_j = -\left(\frac{\eta}{\kappa}\right)(\omega/D)^{1/2}e^{-i\pi/4},\ d = (\omega/D)^{1/2}Le^{-i\pi/4},$$

and D the diffusion coefficient.

The constants $c_{i,j}$ for i,j=1,2, are obtained applying the boundary and continuity conditions.

Finally, the value of pressure given by Equation 9 is substitute in the Equation 4, to obtain the complex effective bulk modulus C*

$$\frac{1}{C^*} = \frac{1}{C_\infty} + \frac{2}{i\omega L}(R_1 - R_2)^2\left(Z_1\cot\left(\frac{d_1}{2}\right) + Z_2\cot\left(\frac{d_2}{2}\right)\right). \qquad (11)$$

The modulus $C_\infty$ corresponds to the high frequency modulus or the no relaxed effective modulus of the media.

The density equivalent to each media, taken into account the solid and fluid is given as

$$\rho_j = \phi_j\rho_{fj} + (1-\phi_j)\rho_{mj},$$

where $\phi_j$ corresponds to porosity, $\rho_{fj}$ to density of the fluid and $\rho_{mj}$ to density of the solid phase of the j-layer.

The density effective to the two layers $<\rho>$, required in Equation 5, is given by $\rho = \frac{d_1}{L}\rho_1 + \frac{d_2}{L}\rho_2$.

Figure 5 represents the attenuation level obtained through Equation 6, with different gas saturation. Observe that in all cases the pick of attenuation is obtained in low frequencies and the higher attenuation is obtained in the case of 15% gas saturation. The values to petrophysical variables are taken from Norris (1993).

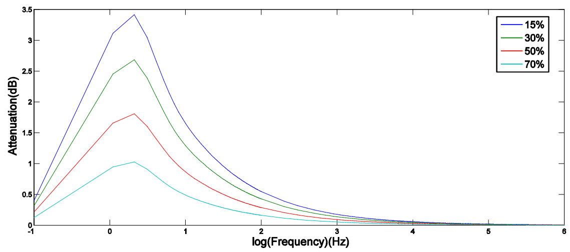


Figure 5: Modeled frequency-dependence attenuation using Equation 6.

**Preliminary Results**

To invert the P-wave attenuation model is necessary estimated the quality factor $\hat{\boldsymbol{Q}}$ from seismic data set. To this end the dataset was processed until Kirchhoff Prestack Time Migration (PSTM) using only the basic processing steps mandatory to avoid process than can modify the relative amplitudes like Radom or Fourier multiple attenuation.

Although the model is based in flat layers, strong lateral $\hat{\boldsymbol{Q}}$ variations can be obtained, because it is estimated trace by trace in the time window selected. The set of common mid points (CMP) from 5710 to 5740 was selected; corresponding to the higher amplitudes of the BSR horizon, see Figure 3.

To obtain the spectra $A(f)$ and $A_0(f)$ at times corresponding to the top and bottom surface of the gas layer, a time-frequency transform is required in each trace. The spectral ratio, using Equation 2, to calculate $\hat{Q}$ via linear regression is reported less sensitive to the choice of bandwidth when wavelet transform is used (Reine et al., 2009).

To this application we need a good vertical resolution in the time-frequency transform, because we need related the spectral amplitude energy at top and bottom of thin layer gas. The better the temporary locations in the time-frequency domain best $\hat{Q}$ values are estimated.

Figure 6, shows the spectral energy obtained to the CMP 5713, using the Gabor time-windowing method and complex continuous wavelet transform (CCWT) using a Morlet wavelet (Cohen et al., 2007). Observe the overall effect of higher frequency suppression more rapidly than lower frequencies.

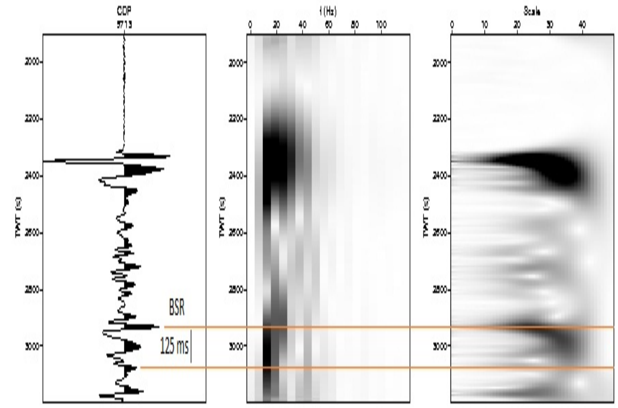


Figure 6: Time-frequency Gabor (left) and CCWT (right) amplitude transform to CMP 5713 trace.

Better time resolution obtained through CCWT is the reason to the selection of this transform to estimation of $\hat{\boldsymbol{Q}}$ values. To compare the two spectra is necessary take into account that the scale in a wavelet transform is inversely proportional to frequency.

A program to select the spectral amplitude to each frequency at the top and bottom horizon of the gas layer was developed. Figure 7 represents three curves of spectral amplitude obtained to the CMP selected with two time windows of thickness 72 ms and 140 ms. The thickness window is around 125 ms, but change in each trace to guarantee the attenuation in the free gas layer. Selecting the time window of 140 ms and using linear regression of spectral ratio, given by Equation 2, was calculated the quality factor $\hat{Q}$, see Figure 8. A value of $\hat{Q} = 67.66$ was obtained in this case.

Through the application of a linear fit approximation of the spectral ratio to each trace, we can produce the input $\hat{Q}$ measured values to fit with the modeled $Q$ in the inversion process. We are developing the inversion process of the objective function, given by Equation 7, limiting the values of the petrophysical parameters with values reported in the literature, as suggested by Morgan et al. (2012).

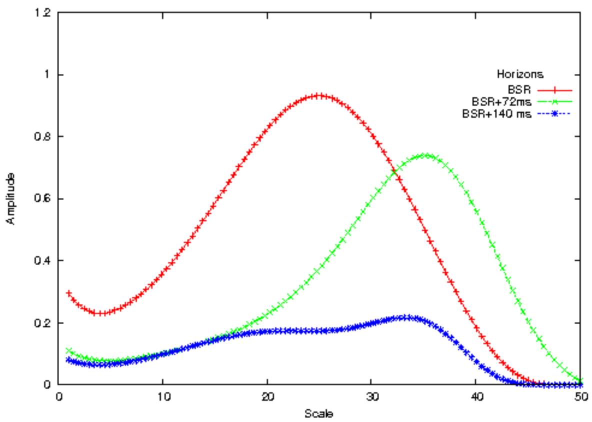


Figure 7: Spectral amplitude obtained in the horizon BSR and two horizons at 72 ms and 140 ms below.

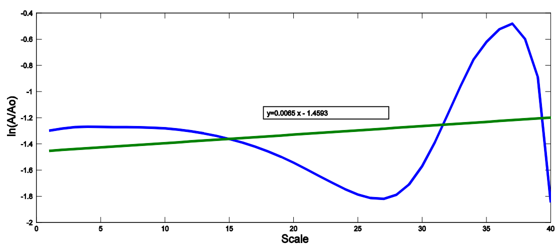


Figure 8: Spectral ratio from BSR and horizon 140 ms below. Linear regression to $\hat{Q}$ estimation.

## Conclusions

Estimation of attenuation values from seismic is a process that can improve the focalization of energy, more adequate AVO analysis and the inversion of petrophysical parameters. In this work the estimation of the quality factor is oriented to estimate the gas saturation through the mesoscopic model of attenuation. Two time-frequency transform was tested to evaluate the spectral ratio, the Gabor and the complex continuous wavelet transform. The time resolution is the more important factor to select the time-frequency transform. The $\hat{Q}$ measured values were obtained to a set of CMP location in a prestack time migrated section. The next step of this work, consisting in the inversion of the $\hat{Q}$ values to estimate the gas saturation is being developed.

## References


Aki, K. and Richards, P., Quantitative Seismology, Vol. I, W.H. Freeman and Company, NY, 1980.

Carcione, J., and Picotte, S., 2006, P-wave seismic attenuation by slow-wave diffusion: Effects of inhomogeneous rock properties: Geophysics, 71(3), O1-O8.

Cohen, J. K. and Stockwell, Jr. J. W., 2007, CWP/SU: Seismic Un*x Release No. 43R3: an open source software package for seismic research and processing, Center for Wave Phenomena, Colorado School of Mines.

Dvorkin, J., and Nur, A., 1993, Dynamic poroelasticity – A unified model with the squirt and the Biot mechanism: Geophysics, 58, 524-533.

Jhonson, D., 2001, Theory of frequency dependent acoustics of patchy-satured porous media: Journal of the Acoustic Society of America, 110, 682-694.

Kumar, N. and Rajput, S., 2011, Exploration of gas hydrates, Geophysical techniques, Springer-Verlag, Berlin.

Liner, C., Elements of Seismic Dispersion, 2012, Distinguished Instructor Series, No. 15, SEG.

Morgan, E., Vanneste, M., Lecomte, I., Baise, L., Longva, O., and McAdoo, B., 2012, Geophysics, 77 (4), R175-R187.

Mueller, T., Gurevich, B, and Lebedev, M., 2010, Seismic wave attenuation and dispersion resulting from wave-induced flow in porous rocks – A review, Geophysics, 75 (5), 75A147-75A164.

Norris, A., 1993, Low-frequency dispersion and attenuation in partially saturated rocks: Journal Acoustic. Soc. Am., 94, 359-370.

Pride, S., Berryman, J., and Harris, M., 2004, Seismic attenuation due to wave-induced flow: Journal of Geophysics research, 109, B01201.

Reine, C., Van der Baan, M., and Clarck, R., The robustness of seismic attenuation measurements using fixed- and variable-window time-frequency transforms: Geophysics 74(2), WA123-WA135.

Zillmer, M., 2006, A method for determining gas-hydrate or free-gas saturation of porous media from seismic measurements: Geophysics, 71 (3), N21-N32.


## Acknowledgments

Funding and data for this research was provided by the Colombian Institute of Petroleum - Ecopetrol. We also thank to University of Pamplona by the research collaboration for this job.